International Journal of Fatigue 33 (2011) 1313–1323

Contents lists available at ScienceDirect

International Journal of Fatigue

journal homepage: www.elsevier.com/locate/ijfatigue

Evaluating the effects of plasma diffusion processing and duplex diffusion/PVD-coating on the fatigue performance of Ti–6Al–4V alloy

G. Cassar [a,*], J.C. Avelar-Batista Wilson [b], S. Banfield [a,b], J. Housden [b], M. Fenech [c], A. Matthews [a], A. Leyland [a]

[a] Department of Materials Science and Engineering, University of Sheffield, Sir Robert Hadfield Building, Mappin St., Sheffield S1 3JD, UK
[b] Tecvac Ltd., Buckingway Business Park, Swavesey, Cambridge CB24 4UG, UK
[c] Department of Metallurgy and Materials Engineering, University of Malta, Msida, MSD 2080, Malta

ARTICLE INFO

Article history:
Received 27 August 2010
Received in revised form 7 March 2011
Accepted 5 April 2011
Available online 12 April 2011

Keywords:
Rotating-bending fatigue
Triode plasma diffusion
Physical vapour deposition
Ti–6Al–4V

ABSTRACT

The effect of triode-plasma enhanced low-pressure oxygen and/or nitrogen diffusion treatments, either as a single process or in conjunction with plasma-assisted physical vapour deposition (PAPVD) on Ti–6Al–4V has been studied under rotating-bending fatigue testing. Following the diffusion treatment, samples exhibit a hardened case, more than 30 μm deep. Semi-logarithmic *S–N* plots are used to demonstrate and compare the significant changes in fatigue resistance obtained from each process. Fractography and residual stress measurements show that, compared to annealed samples, the fatigue strength of the diffusion-treated samples was superior; although the result changed depending on the processing parameters and microstructure of the substrate material. Also, unsupported and mechanically uncompliant ceramic coatings, such as TiN, promote the initiation of multiple crack sites, which lead to premature failure of the Ti-alloy substrate and a consequent reduction in endurance limit.

1. Introduction

Titanium and its alloys are now widely used in industry due to their high strength-to-weight ratio, high corrosion resistance and excellent biocompatibility. However, it is well known that the tribological performance of such materials in contact with counterface materials is extremely poor [1–3].

Over the last two decades a wide range of surface engineering processes have been developed to improve the tribological properties of titanium alloys. Diffusion treatments and particularly techniques which use intensified-plasma processing have proved to be particularly efficient. Such low-pressure vacuum processing methods are effective as a substrate pre-treatment, prior to subsequent deposition of wear-resistant PVD ceramic coatings [4–6]. These Duplex or Hybrid techniques are based on the principles of substrate pre-treatment to improve the mechanical load bearing capacity. Then, a suitable tribological hard coating is applied to increase wear resistance [7,8].

Titanium is also very commonly used when fatigue resistance is key to the survivability of the product. As a result, surface treatments which are originally designed to improve tribological behaviour should also not reduce the fatigue strength of the base material. While the tribological behaviour of similar treatments was studied recently in [9], the following discussions are focused primarily towards the effect of such treatments on fatigue behaviour. Unfortunately, there is little work on the effect of surface engineering treatments on the fatigue performance of Ti-alloys and particularly the effect of triode plasma diffusion treatments has not yet received detailed attention. Costa et al. [10] have shown a reduction in fatigue strength for PVD TiN coated Ti–6Al–4V, while Wilson et al. [11] reported an improvement in the endurance limit of PVD coated and duplex-treated Ti–6Al–4V. Similarly, there are conflicting reports in the literature regarding the effects of thermochemical conversion treatments, such as oxidation [12] and nitriding [13], on the fatigue limit. Grain growth, changes in crack initiation and growth resistance and the presence of flaws in surface compound layers and coatings have been related to the observed changes in fatigue performance.

In this work, rotating-bending fatigue strength of Ti–6Al–4V nitrided and oxynitrided by novel triode plasma diffusion processes and Ti–6Al–4V alloy TiN coated by an electron-beam (EB) PAPVD was evaluated. Ti–6Al–4V was chosen because of its widespread aeronautical application. Therefore, any capability to improve its tribological properties without affecting bulk mechanical behaviour is important. Microhardness depth profiles, rotating-bending fatigue tests, post-failure fractographic inspection and XRD residual stress measurements were used to analyse the effects of the various plasma-assisted treatment combinations on fatigue strength and primary failure mechanism.

* Corresponding author. Tel.: +356 2340 2140; fax: +356 2134 3577.
E-mail address: glenn.cassar@um.edu.mt (G. Cassar).

0142-1123/$ - see front matter © 2011 Elsevier Ltd. All rights reserved.
doi:10.1016/j.ijfatigue.2011.04.004

2. Experimental details

The nominal chemical composition of the (annealed and air cooled) Ti–6Al–4V alloy used was 6.01 wt.% Al, 4.08 wt.% V, balance Ti. The base material was diffusion-treated by plasma nitriding or combined oxidising/nitriding in a modified Tecvac IP70L commercial coating system, using a low-pressure D.C. triode configuration [4,14] and additional radiative heating.

Two groups of specimens, untreated or pre-nitrided, were coated with TiN by EB-PAPVD. The grounded chamber served as an anode for the discharge while the samples and holding fixtures formed the principal cathode. Thermionic plasma enhancement was provided by an additional electron-emitting cathode in the form of a hot tungsten filament, biased at −200 V, positioned near the base of the chamber.

Triode enhanced-plasma diffusion treatments were carried out for a total of 4 h in a mixture of 70% partial pressure of nitrogen or oxygen and 30% partial pressure of argon, at a total gas pressure of 0.4 Pa. TiN was deposited by EB-PAPVD using a Tecvac IP70L coater. During coating substrate temperatures ranged between 400 and 450 °C. Samples were firstly diode sputter cleaned in Ar at ~2 Pa chamber pressure and 1000 V substrate negative bias, then a thin Ti interlayer with a thickness between 0.1 and 0.2 μm was deposited under a pressure of 0.3 Pa and triode conditions. Finally, a TiN ceramic coating layer was deposited for approximately 100 min, to give a thickness of 2.8 ± 0.2 μm.

The test coupons used included flat discs which have dimensions of 30 mm diameter and 4 mm in thickness and core hardness of 375 ± 10 $Hk_{0.025}$, polished to a mirror finish of R_a = 0.03 ± 0.01 μm. Similarly, rotating-bending fatigue specimens were prepared and subsequently treated under identical process conditions.

A stress relieving cycle was also carried out to provide a neutral benchmarking sample for comparison. This consisted of heating to 600 °C and a dwell of 1 h, under vacuum. Then, the sample was furnace cooled at a rate slower than 2 °C/min [15].

2.1. Characterisation

Knoop microindentation hardness measurements were performed on polished substrate cross-sections using a Mitutoyo HM microhardness tester, set at a load of 25 gf (1 gf = 9.81 mN) and a 20 s dwell time. The test method used followed the relevant standard for Knoop hardness testing of metallic materials – BS EN ISO 4545-1:2005 [16]. The first indent impression was positioned at a distance >8 μm from the surface to minimise the effects of the unconstrained surface buckling under load. Surface nanoindentation measurements were performed using a Hysitron Inc. Triboscope™ equipped with a Berkovitch triangular-pyramidal diamond indenter with an approximate average radius of curvature of 150 nm. Fifteen indentations were made for each sample at a constant maximum indentation depth of ~100 nm for coating measurement and ~50 nm for diffusion-treated samples. Corresponding maximum loads of around 10 mN and 5 mN were used for coatings and diffusion-treated samples, respectively. The use of nanoindentation allowed the determination of local hardness values without significant substrate contribution to the measured results. For consistency, Knoop cross-sectional hardness values have also been converted to GPa.

A Veeco Dektak 3^{ST} stylus profilometer was used for measuring surface roughness values. Five measurements (at random positions and orientations) were recorded to calculate an average R_a value. The 12.5 μm radius stylus tip was loaded with a load of 30 mg and the scan duration was set such that the traversing resolution was better than 0.05 μm. The vertical resolution was less than 0.01 μm.

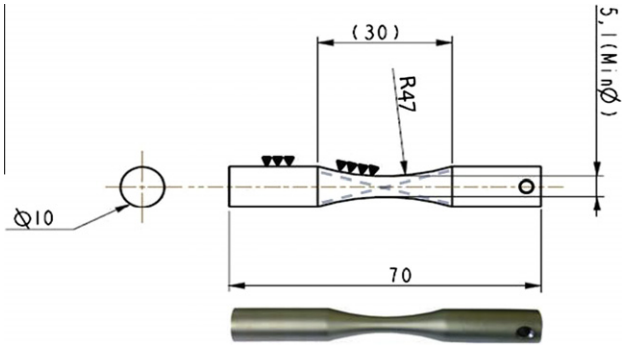

Fig. 1. Schematic drawing of fatigue test sample geometry (dimensions are in mm) and a photographic image of a typical finished specimen.

2.2. Rotating-bending fatigue tests

Ti–6Al–4V as-received rod material with a diameter of 10 mm was prepared according to Fig. 1. The test sections of specimens were polished using metallographic techniques to a roughness of 0.04 ± 0.01 μm R_a. Polishing was used to remove circumferential machining marks and to ensure an 'identical' surface for all samples prior to plasma surface treatment, as dictated by the relevant standard BS 3518-2 (1962) [17].

Fully-reversed tensile–compressive stress cycling was performed using an Italsigma 2TM831 rotating-bending fatigue test machine, applying a sinusoidal loading regime at a frequency of 50 Hz and a loading ratio of $R = -1$. The test method, including the sample set up routine, was in accordance with recommended procedures outlined by Italsigma and the standard practice for conducting such experiments is presented in [17]. Each test ended either when the sample ruptured or when the number of cycles reached 10 million. The pre-determined number of cycles to run-out was arbitrarily chosen in accordance with standard practice to limit the maximum duration of the test. A minimum of 14 samples for each type was tested, although in most cases up to 20 were used. This allowed a sufficient number of replicate tests to achieve a percent replication (PR) value between 55% and 70%. The median *S–N* and staircase methods were employed for the determination of the fatigue life and fatigue limit respectively, according to BS ISO 12107:2003 [18].

Table 1 provides a summary of the process parameters and chosen designation for the samples tested. The table also lists two reference samples used for benchmarking the effect of the process. The plasma annealed samples were treated in an identical triode plasma nitriding (TPN) process at 700 °C; however, they were protected from the bombarding energetic species by each sample being individually wrapped in a thin stainless steel foil capsule. After treatment the samples were cooled slowly inside the furnace. These samples were therefore subjected to the same thermal cycle experienced by a plasma diffusion-treated sample (to obtain an identical 'post-treatment' bulk microstructure), whilst at the same time retaining the surface condition (chemistry and topography) of the untreated alloy material. Following the test the fracture surfaces of the fatigue samples were examined by optical stereomicroscopy and scanning electron microscopy (SEM).

2.3. X-ray stress analysis

A Siemens D5000 diffractometer (Cu K_α radiation) was used for surface stress analysis. The tube acceleration voltage and current used were 40 kV and 30 mA respectively. Glancing-angle X-ray diffraction (GAXRD) patterns were used to identify the best candidate peaks; α-Ti(1 0 3) at $2\theta = 71.6°$ and α-Ti(2 1 1) at $2\theta = 109.1°$

Table 1
Ti–6Al–4V samples selected for fatigue testing.

Group	Designation	Diffusion treatment processing parameters			
		Cathode bias (V)	Duration (h)	Working gas	Temperature (°C)
Reference	Untreated	–	–	–	–
	(Plasma) Annealed	–	4	–	700
Diffusion Treated Only	LV-TPN	−200	4	N_2	700
	LV-TPN(HT)	−200	4	N_2	800
	LHV-TPN	−200	3	N_2	700
		−1000	1	N_2	700
	LHV-TPON	−200	1	O_2	700
		−200	2	N_2	700
		−1000	1	N_2	700
Duplex	LHV-TPN + TiN	−200	3	N_2	700
		−200	1	N_2	700
Coated Only	TiN	–	–	-	–

LV denotes Low Voltage, LHV represents a Low Voltage stage followed by a High Voltage stage and HT signifies a High Temperature process.

appeared most suitable for the stress measurement procedure. Next, the Bruker-axs Edstress program was used to set up the parameter files for the measurement. The Bruker-axs Diffrac^{plus} software was used to calculate the normal and shear stresses, according to the procedure outlined in the Bruker-axs Advanced Residual Stress Determination manual.

Nine ψ angles ranging from −45° to 45° were used, with a step size of 0.01° and an exposure time of 60 s applied. Before determining stress tensor components, the Diffrac^{plus} software also allowed various intensity corrections to be made; including the removal of background signal noise, of the effects of $K_{\alpha 2}$ radiation from the tube and also 'smoothing' (i.e. moderating the effects of counting statistics). The centre of gravity method was selected to determine the (shifted) peak position. This method utilises the intensity distribution of a diffraction line above an intensity threshold, which in this case was set to 10% and calculates its angular centre of gravity thereby determining the peak position.

3. Results and discussion

3.1. Hardness profile

Hardness-depth profiles, shown in Fig. 2, indicate the effect of the different treatment combinations. The diffusion of oxygen and nitrogen during the 4 h process clearly increases the hardness of the Ti–6Al–4V samples considerably, while below the hardened case no change in the substrate hardness can be observed. As expected, the degree of hardening and effective case depth increase rapidly at higher temperatures. The higher solute diffusion rate for LV-TPN(HT) at 800 °C compared to that of LV-TPN at 700 °C leads to a measurable increase in hardness at up to 60 μm treatment depth in the former compared to around 30 μm in the latter.

Fig. 2 also shows that the surface hardness increased from 3.8 GPa to 15 GPa and 9.2 GPa following treatment at 800 °C and 700 °C, respectively. The increase in surface hardness results from the formation of a compound layer comprising Ti_2N and TiN. This compound layer was 1.65 μm thick at the higher treatment temperature of 800 °C compared to 0.18 μm following treatment at 700 °C.

The introduction of 1 h of nitriding at a high negative bias voltage in the later stage of LHV-TPN does not measurably improve the overall hardness-depth profile in the treated Ti-alloy substrate. Nevertheless, this contributes to an increased near-surface hardening by promoting nitride compound-layer formation. The low-pressure intensified glow discharge used for nitriding permits the arrival of very high numbers of energetic ionised species carrying almost the full cathode fall potential [19]. These ions have a mean energy well in excess of the minimum particle energy necessary to initiate vacancy generation in TiN (∼200 eV) [20] and also exceed the minimum energy required for a nitrogen ion to become trapped inside a metal lattice (∼150 eV) [21]. The effect of using a higher cathode bias on surface hardness is difficult to measure due to a combination of surface roughening and unavoidable substrate contributions to the measured values. However, although the effect on surface hardness was apparently marginal, nanoindentation did show an increase in surface hardness from ∼9.3 GPa in LV-TPN to ∼10.2 GPa in LHV-TPN. This final hour of high-voltage nitriding in the latter process not only improved the load-support for the subsequently deposited TiN layer by creating a more gradual change in mechanical properties (Fig. 2b) but also improved coating adhesion due to better chemical compatibility.

The introduction of the HV parameters in the later stages of the process and its deliberate avoidance in the early stages is dictated by two considerations:

(i) Nitride surface compound layer thickness increases with the treatment bias voltage [9]. The coefficient of diffusion of nitrogen in TiN and Ti_2N is at least 30 times lower than for α-Ti [19,22] and therefore the compound layer act as a diffusion barrier for further nitrogen penetration into the bulk. If introduced too early in the treatment process this may significantly reduce the overall case depth achieved.
(ii) Extended HV processing has been proven to create a significantly rougher surface because of increased and selective sputter etching. Rougher surfaces act as a source of hard, abrasive wear debris and thereby degrade the tribological performance [9].

Additionally, the first hour of triode plasma nitriding was replaced with an oxidation step (TPON, Table 1). The rate of oxygen diffusion in α-Ti is known to be much higher than that of nitrogen at a given temperature [22,23] and, more importantly, can be maintained at its maximum potential – irrespective of whether or not a compound layer is formed at the surface during the oxidation process. In fact, the diffusion coefficient for oxygen in rutile TiO_2 is – unlike nitrogen in TiN/Ti_2N – about 50 times higher than in Ti(O)-metal at the same temperature [23]. In other words, an oxide compound layer will not inhibit the growth of the solid solution strengthened zone over time and therefore the case depth achieved will be deeper when compared to an equivalent nitriding process.

The subsequent nitriding steps incorporated into the TPON treatment act to boost-diffuse the oxygen from the oxide layer into the bulk thereby consuming any residual oxide compound layer generated on the oxygen pre-treated alloy surface. This step also diffuses nitrogen into the near surface to increase hardness, and improve 'chemical compatibility' with the PVD coating. These

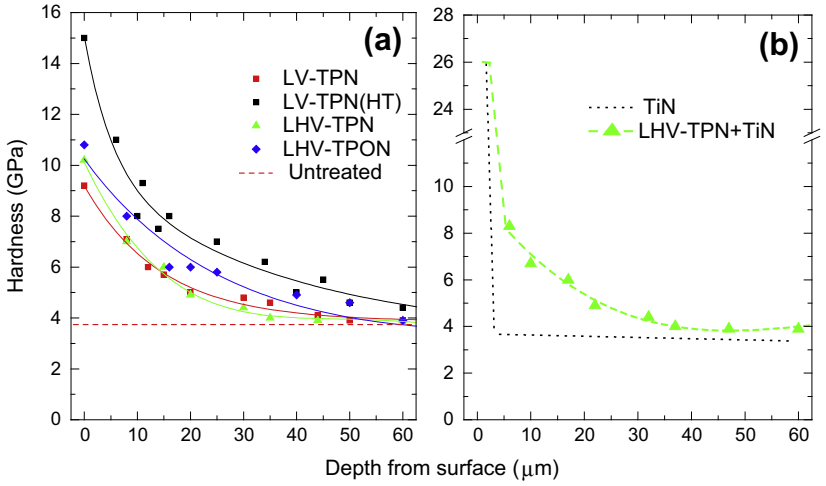

Fig. 2. Hardness–depth profiles of (a) diffusion-treated and (b) duplex treated/coated samples. Note: Curves shown have been plotted using allometric and exponential data fits and are only intended to help the reader differentiate between hardness profiles.

latter points are extremely important since a TiN PVD coating would not adhere well to an oxide compound layer. Three hours of nitriding was found to be sufficient to completely consume any oxide formed. Scratch tests [24] performed on duplex TPON oxy-nitrided/PVD coated samples showed no degradation in the measured critical loads for coating cohesive and adhesive failure, compared to nitriding alone.

3.2. Fatigue test results

The rotating-bending fatigue results obtained for the triode plasma diffusion-treated samples are presented in the form of *S–N* semi-logarithmic graphs in Fig. 3. These have been plotted according to the graphical presentation method outlined in ASTM standard E468-90 [25], i.e. by applying regression analysis to the numerical data. For all samples, the correlation coefficient obtained through the analysis of variance indicates very good agreement between the linear fit and the test data. The variables of the regression function, together with the statistical measures of the data dispersion are also provided in Table 2.

The rotating-bending fatigue results for the untreated substrate material shows an endurance limit of around 800 MPa [26,27] and

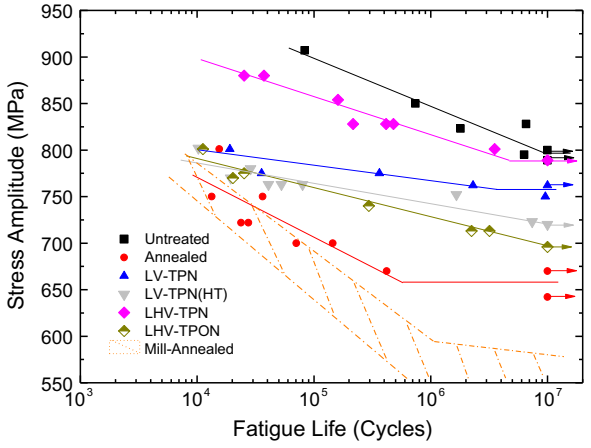

Fig. 3. *S–N* diagram for reference and diffusion-treated samples. Arrows indicate samples that did not fail. Region marked for mill-annealed microstructure comprises fatigue data from [30,33,34].

tests carried out on triode plasma diffusion treated samples indicate a strong relationship between fatigue performance and diffusion treatment depth. The reduction in fatigue strength of diffusion treated specimens becomes more significant as the efficacy of the diffusion process improves. This behaviour confirms previous studies in which diffusion case thickness has more influence on fatigue resistance than compound layer formation [28,29].

It is well known that the fatigue strength of titanium is very sensitive to changes in morphology and arrangement of the two constituent phases, α and β [30]. In fact, the change in fatigue strength of the untreated material compared to that of the annealed material is very significant. The endurance limit of the former was 798 MPa and, following plasma annealing cycle (Table 1), decreased to 658 MPa i.e. a reduction of around 18%.

The conditions under which annealed samples were prepared indicate that it is primarily the change in substrate microstructure caused by exposure to the heat cycle that reduces the fatigue life of triode plasma treated samples. Indeed, the respective *S–N* plots of all the diffusion-treated samples fall within the range bounded by these two reference samples. This implies that, compared to the annealing treatment alone, the various plasma diffusion treatments actually impart a net improvement in fatigue strength.

Fig. 4 shows optical micrographs of the structure of the as-received (untreated) substrate material, which is composed of fine intergranular β in an α matrix. The α–α grain boundaries are not well defined; however, the grain dimensions can be approximated to have a mean length (along the major axis) of ~5.1 μm and a width of ~1.1 μm. The annealing process (which is essentially an isothermal treatment for 4 h at 700 °C; except for sample LV-TPN(HT); see Table 1), applied to the bulk material during any of

Table 2
Variables of regression function: $S = A + B \log(N)$, describing the finite fatigue life range of *S–N* plots.

Sample ID	Constant, *A*	Constant, *B*	Standard error	Correlation coefficient
Untreated	1149.2	−21.9	16.3	0.94
Annealed	1028.8	−28.1	24.1	0.83
LV-TPN	851.7	−6.2	11.2	0.83
LV-TPN(HT)	865.5	−8.8	10.9	0.89
LHV-TPN	1054.5	−17.2	8.5	0.97
LHV-TPON	920.1	−14.1	8.5	0.98
LHV-TPN + TiN	1334.5	−43.5	14.6	0.94
TiN	1471.7	−61.58	21.4	0.92

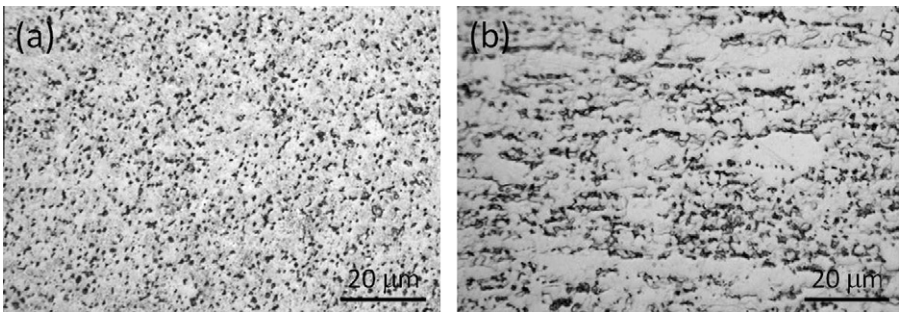

Fig. 4. Micrographs of (a) transverse and (b) longitudinal sections of the as-received (untreated) microstructure of the Ti–6Al–4V material used to manufacture fatigue specimens.

the triode plasma diffusion treatment, explains the substantial microstructural changes observable in the alloy substrate after plasma treatment. Following the treatment, the structure formed changed depending on the duration of the diffusion process. After two hours a bimodal structure emerges [30], with primary α embedded in a lamellar $\alpha + \beta$ matrix (Fig. 5a and b). Extended annealing (i.e. longer diffusion treatments), and particularly treatment LV-TPN(HT) carried out at 800 °C, led to increased growth of the α lamellae with remaining β-phase restricted to the grain boundaries, as shown in Fig. 5c.

From tensile testing of as-received, annealed and diffusion-treated cylindrical bars [24], the Hall–Petch related reduction in yield strength observed is clearly significant; however, finer microstructures are also associated with a retardation in crack nucleation [31]. In this case, where the material is practically defect-free before the test, the lifetime of the samples is dominated by this annealing component. Furthermore, the change in fatigue behaviour of the material following treatment has to be related to possible differences in prevalent initiation sites and in microcrack propagation rates between the as-received fine microstructure and the resulting bimodal microstructure [32]. It is also worth mentioning that the observed 18% reduction in strength is most likely exaggerated by the original very fine microstructure. For components of larger cross-section, with a (more typical) mill-annealed microstructure, it is plausible to predict an almost negligible change in fatigue life of a substrate already annealed at 700 °C (and consequent improvements following diffusion treatment). In fact, Fig. 3 also includes literature data [30,33,34] for similar tests performed on samples having a mill-annealed microstructure and clearly, the results are inferior to all plasma treated variants. However, irrespective of the initial microstructure, better control of post-treatment cooling rate (from the $\alpha + \beta$ phase field) may be appropriate in order to optimise bulk microstructure. Nitriding process routes similar to that suggested by Major et al. [35] may be adopted in order to maximise substrate fracture toughness.

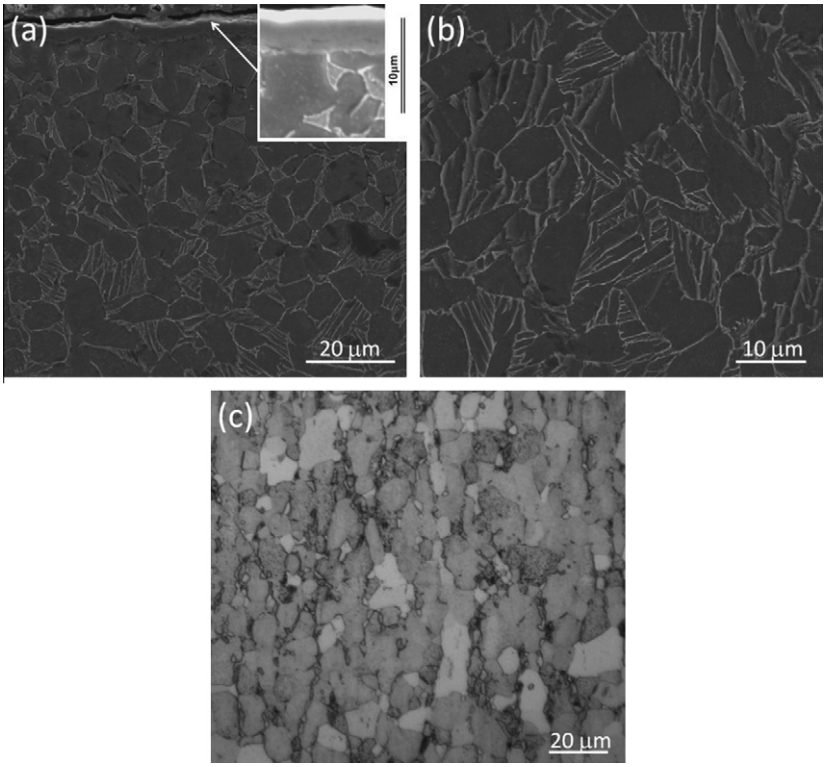

Fig. 5. Micrographs (a) and (b) show the biomodal microstructure of material used for fatigue specimens following nitriding at 700 °C for 2 h. (a) shows the transition from the bulk to the surface – insert shows subsequently deposited TiN coating on top of the compound layer formed during the diffusion process, while (b) shows the bulk microstructure. (c) shows the bulk microstructure following HT treatment at 800 °C for 4 h where finer β grains remain only at the grain boundaries of the larger α grains.

Fig. 3 shows that all four types of sample exhibit an improved mechanical response to cyclic loading compared to the annealed samples. It becomes clear that the fatigue strength can be improved by triode plasma diffusion treatment to a level almost on a par with that exhibited by the atypical, very fine microstructure of the as-received material. Again, considering a 'defect-free' condition before the test, fatigue crack initiation becomes the critical stage which dictates the fatigue life. Thus, surface treatments have the potential to play a key role in determining fatigue behaviour, particularly since the surface, where damage accumulates due to plastic strains several times larger than in the bulk [36], is the most likely origin of fatigue cracks. The improvement in fatigue life can be attributed to surface strengthening associated with the reduced mobility of dislocations and therefore the inhibition of slip step formation, together with the presence of a compressive residual stress state at the surface (due to lattice strain induced by interstitially-located nitrogen and/or oxygen). While both these effects reduce the generation of surface and subsurface cracks, the latter also suppresses the propagation of such cracks, which may otherwise lead to failure.

The delayed micro-yielding and generation of compressive stress are both enhanced in triode plasma processes, particularly when compared to 'non-intensified' treatment regimes. Therefore, the results point towards the inherent suitability of intensified processes if fatigue performance is considered critical for the intended application. In fact, conventional gas nitriding processes are known to reduce the fatigue limit of titanium alloys [37]. The higher treatment temperature, typically exceeding 900 °C, accelerates solute diffusion but may not be conducive to the retention of substrate core strength. Thus the ability to surface harden components at temperatures as low as 700 °C (i.e. significantly below the β transformation temperature) is crucial in minimising bulk microstructural changes.

In the literature, nitriding of titanium alloys performed at high temperature was reported to create a hard brittle layer which reduced crack initiation resistance and thus led to premature failure and a resultant drop in fatigue strength [13]. Conversely, the triode process used in this work improves the fatigue life due to minimal grain coarsening, residual compressive stress introduced by interstitial solid solution and a gradual change in mechanical properties from the surface to the bulk [19,20]. The nitride compound layer formed in gas nitriding of titanium alloys (performed at high temperature) is unlikely to provide such effects and the fact that its removal improves the fatigue strength [13] implies that the hard brittle layer tends to act as an additional source of fatigue cracks and may thus contribute to premature failure.

As highlighted in the discussion above, a higher nitriding temperature has a more pronounced detrimental effect on fatigue strength and the 800 °C LV-TPN(HT) treatment does indeed exhibit a slightly worse performance, compared to its 700 °C LV-TPN equivalent. Any strengthening enhancement obtained at 800 °C is counteracted by the much higher degree of grain coarsening (Fig. 5c). Accelerated grain growth is often reported for nitrided samples treated above 900 °C [38] and therefore treatments at temperatures approaching this value are likely to exhibit an overall inferior performance.

Examination of the fatigue results presented for LHV-TPN shows that the final hour of triode plasma nitriding at a high substrate negative bias (−1000 V) also appears to have a substantial positive contribution to the fatigue performance of the test specimens. Owing to the intensified-plasma system used, the ionic species arriving at the surface during the treatment have relatively high energies and therefore enhance both re-sputtering and subplantation processes. The resultant increase in supersaturation of the Ti alloy with nitrogen also raises the residual compressive stress in the surface.

In this work, all samples were diffusion-treated for a total of 4 h since this was considered the minimum time necessary to provide a tribologically effective case depth and allow differences between the different treatment regimes to be clearly distinguished. It is expected that increasing the cycle time to between 6 and 8 h could provide a net improvement in fatigue properties when compared to the as-received high-fatigue-strength alloy condition. Recent work on plasma carbonitriding of $\alpha+\beta$ Ti–6Al–2Cr–2Mo alloy [39] showed a progressive improvement in fatigue strength with increasing treatment time (in the range of 3–12 h), compared to an annealed equivalent. Furthermore, GAXRD stress analysis of flat coupons subjected to an 8 h version of the LHV-TPN process yielded a threefold increase in compressive residual stress compared to a 4 h process, resulting in a normal stress in excess of 1.2 GPa at the surface. However, it has also been demonstrated that any detrimental effects on cyclic fatigue performance of similar engineering treatments can be accentuated with increasing treatment duration [6,13,40] as recrystallisation and grain growth take place. In this respect, the short processing times used in this work are considered beneficial.

Finally, in order to illustrate the effect of introducing oxygen in the process cycle the data of LHV-TPN can be contrasted with the results presented for LHV-TPON (Fig. 3). These two processes are identical except that in the latter the first hour of nitriding was replaced by a pre-oxidation stage. Consequently, the less marked improvement in fatigue life (compared to the baseline annealed substrate condition) has to be explained by the difference in diffusion kinetics between oxygen and nitrogen under otherwise identical conditions. This can be attributed to two principal factors: (i) titanium is able to dissolve a larger quantity of oxygen than nitrogen (~31 at.% O vs. ~10 at.% N at 700 °C [41]) and therefore once the sample has cooled the resultant degree of supersaturation is less for the former; and (ii) lattice strain induced by oxygen located (mainly) in the octahedral sites of the hcp α-Ti structure is significantly lower for the same atomic content compared to nitrogen, both perpendicularly and along the basal planes [42]. As a result, less distortion is induced by oxygen located interstitially in the titanium lattice, and therefore lower levels of residual compressive stress are created. Also, the suppression of dislocation activity and associated slip mechanisms due to oxygen uptake is less intense than by nitrogen – even if the oxygen content is comparatively high.

3.3. Residual stress analysis

The normal stresses measured using the $\sin^2\psi$ method are shown in Fig. 6. The results presented for nitrided samples validate the above discussion. Clearly, the triode plasma nitriding and oxynitriding treatments create direct compressive stresses at the surface of the treated Ti alloy, which could be of significant importance to the fatigue behaviour of Ti–6Al–4V since they effectively reduce the maximum surface tensile stress experienced during the rotating-bending tests [43]. This normal stress is also accompanied by low-magnitude shear stresses; however, these have been observed to vary only slightly between all diffusion treated samples and typically lie between 55 and 85 MPa. In comparison to LV-TPN, both LV-TPN(HT) and LHV-TPN result in a higher normal stress as the degree of supersaturation of nitrogen is greater following treatment. The residual stress generated by the LV-TPN(HT) was the highest observed; nevertheless, this presented lower fatigue resistance due to degradation in bulk mechanical properties as a result of the grain growth that occurred at 800 °C.

At the surface, LHV-TPN and LHV-TPON presented similar surface compressive residual stress, considering standard deviation. This stems primarily from the fact that XRD stress measurement is essentially a near-surface characterisation technique and

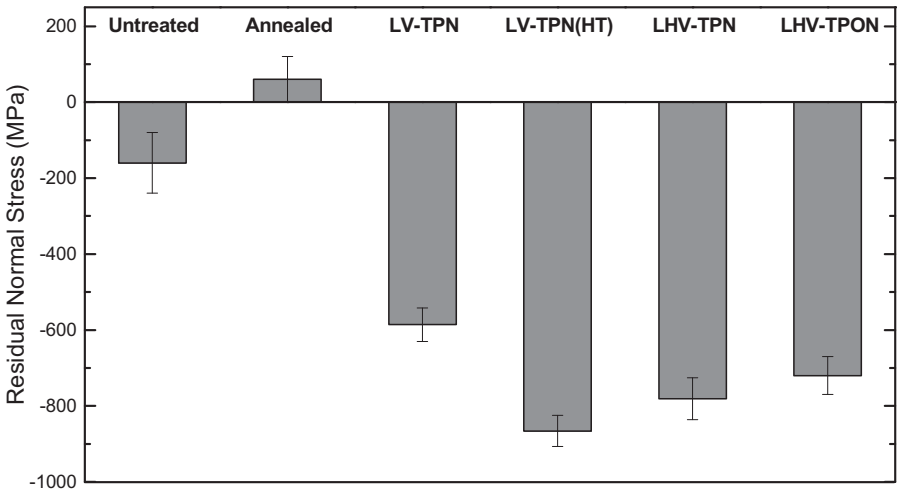

Fig. 6. Normal surface stresses for Ti–6Al–4V samples measured using XRD $\sin^2\psi$ method.

although X-rays do penetrate several microns into the material, the measured lattice strain (and in turn the stress) is in effect averaged over only a thin surface layer [44]. Thus, the technique is not suitable to compare samples which, albeit subject to different processes, are essentially identical in the near surface region, such as LHV-TPN and LHV-TPON. Unfortunately, successive material removal methods could not be used to generate and then compare stress–depth profiles. Typically, these tests have a step resolution of say 50 μm, i.e. much larger than the case depth of interest in this work.

Fig. 6 also shows the stress measured for untreated and annealed material. The untreated samples overall had some degree of compressive residual stress which was probably introduced by Hertzian and shear forces imparted during grinding and polishing. Conversely, some of the annealed samples showed a direct tensile stress. This was probably generated by heating and cooling during the thermal cycle needed for the diffusion process. Unfortunately, the results were found to vary substantially as a result of non-identical cooling rates between runs. This is common for diffusion treatments whereby the cooling rate under vacuum, from treatment temperature, is relatively high (for example, in the cases of TPN/TPON treatments more than 3 times that used in a typical stress relieving process).

3.4. Fracture topography

It has been reported that thermochemical processes, such as nitriding, and mechanical surface treatments such as roller burnishing, can induce subsurface fatigue crack nucleation [45–49]. This has been attributed to the compressive–tensile stress profile generated below the surface of the material. For untreated and annealed samples cracks were expected to originate from the surface. Conversely, for samples which had been triode plasma diffusion-treated and tested in high cycle fatigue subsurface cracking could occur. It has also been reported that differences in the point at which crack initiation is related to the maximum bending stress applied and therefore the duration of the test [33]. More recently, Torres and Voorwald [50] suggested that, in low cycle fatigue, the high tensile load applied will always surpass any compressive residual stress present – thereby favouring surface cracking. From the fractographs observed, the distinction between surface and subsurface crack initiation was not always easily identifiable. For triode plasma treated samples this was mainly attributed to the relatively shallow case depth of a number of the samples evaluated.

Indeed, longer lifetime tests (carried out at moderate levels of applied stress) typically exhibited subsurface crack origins, an example of which is shown in Fig. 7a, while a higher applied stress activated multiple surface crack initiation sites which ultimately led to the formation of visible radial ratchet marks (i.e. step-like junctions between adjacent fatigue cracks), Fig. 7b. The topography of the remaining bulk portion of the samples did not vary much and consisted principally of (i) a region of slow crack propagation characterised by fatigue striations and some secondary intergranular fissures (Fig. 7c) and (ii) a smaller region of ductile tensile yielding and instantaneous overload fracture, characterised by a mixture of dimpled ruptures and tear ridges (Fig. 7d).

Overall, the fatigue crack propagation surface was more uneven in all diffusion-treated samples compared to the equivalent fractures in the untreated material. The formation of more jagged fracture surfaces can be attributed to the coarser microstructure of the heat-treated compared to the as-received material. Other surface characteristics of the 'slow fracture' zones that were observed include occasional macro-progression ('beach') marks and some 'river' marks, showing the direction of progression of the fatigue cracks laterally towards the instantaneous fracture zone.

3.5. Coated and duplex treated samples

Fig. 8 shows experimental results for the samples which have been coated with TiN – both duplex diffusion/PVD and only PVD-coated samples. The data presented for PVD TiN-coated samples shows a substantial degradation in the fatigue performance of all samples, whether diffusion-treated or not. However, the reduction in endurance limit in the material diffusion-treated prior to PVD coating was only around 5% compared to around 25% for the TiN coating on the untreated substrate. This is of particular relevance when considering that the thin film deposition process (i) is carried out at only 400–450 °C and therefore there is no effect on the substrate microstructure and (ii) unlike some of the triode plasma diffusion processes, negligible surface roughening occurs. Clearly, the drop in fatigue life has to be directly related to the presence of a hard, high-modulus layer at the surface of the sample. Although, this layer is composed of similar ceramic nitrides to the compound layer generated during nitriding, the TiN deposited by PVD is both significantly thicker than the TiN/Ti_2N compound layer and also has a well defined columnar morphology. For columnar coatings, any crack normal to the surface can become large in a thick coating thereby exceeding the critical crack length. Conversely, in a thin coating (or hard compound) this may not be possible [51,52].

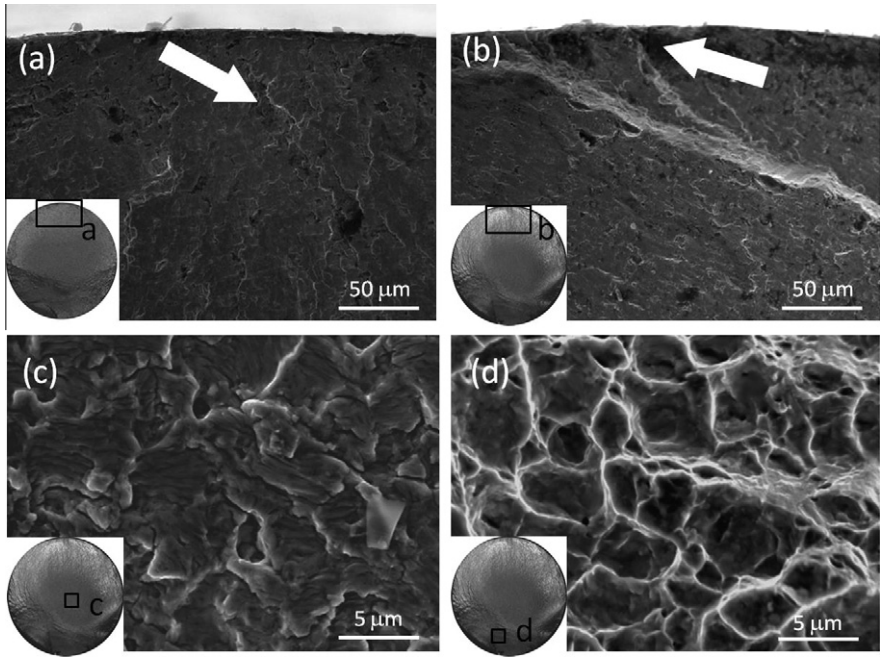

Fig. 7. SEM micrographs of LHV-TPON-treated Ti–6Al–4V fracture surfaces. Sample 1: (a) Tested at a stress amplitude of 700 MPa and survived around 4.1 million cycles – showing sub-surface crack initiation. Sample 2: (b) Tested at a stress amplitude of 800 MPa and survived around 0.01 million cycles – showing surface crack origin; (c) fatigue striations and numerous secondary cracks away from origin at the surface; (d) ductile failure region exhibiting tensile dimpling.

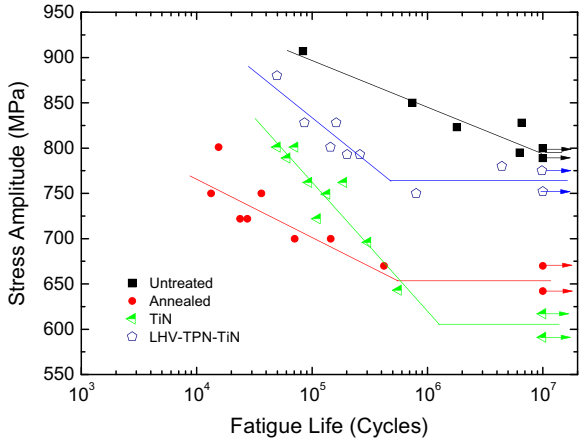

Fig. 8. *S–N* diagram for reference and coated samples. Arrows indicate samples that did not fail.

Cracks are more readily initiated in the ceramic coating due to the inability of the much stiffer coating layer to withstand the elastic strain imposed by substrate deflections under load [53]. Also, local defects, such as voids and inclusions, are known to act as crack initiation sites [50,54]. Furthermore, particularly if adhesion of the coating to the substrate (or to the diffusion-treated layer) is not sufficiently high, fatigue cracks have been proved to originate at the coating-substrate interface [55,56]. For the work presented in this paper, fracture cross-sections and scratch adhesion measurements [24] of TiN-coated Ti–6Al–4V coupons prove that the deposited TiN coatings are dense and well adhered.

Nevertheless, delamination can still occur due to the substantially different elastic moduli of the substrate and coating (~5–6 times higher for the latter [57]) which leads to strains that cannot be endured by the TiN layer. Clearly, such effects are amplified at higher stress amplitudes, where the surface strain is particularly high. Fracture surfaces of TiN-coated Ti–6Al–4V are presented in Fig. 9a tested at 640 MPa and Fig. 9b tested at 800 MPa. When a lower stress is applied, Fig. 9a shows a single crack initiation point while at a higher stress amplitude a number of ratchet marks are generated between several crack origins (Fig. 9b). The ratchet marks are indicative of multiple crack fronts which rapidly progressed from the surface into the bulk leading to premature sample failure at ~49,000 cycles.

In regard to other fatigue-related studies of PVD TiN-coated materials, it is clear that the substrate elastic modulus (and therefore the degree of coating/substrate modulus mismatch) has an important influence on the observed results. Other authors [58,59] who used steel as the substrate material were able to show an increase in endurance limit following TiN deposition. This is also in agreement with recent work by Baragetti et al. [53] who demonstrated similar differences in examining the effect of CrN coatings on fatigue limit. Coated specimens exhibited a fatigue life increment for stainless steel and tool steel but a slight decrement was observed in the case of aluminium when tested using rotating-bending fatigue tests at the maximum applied bending stress of 600–845 MPa.

Fig. 8 also reveals that the percentage reduction in fatigue life of only TiN-coated samples compared to the untreated substrate increases with decreasing stress level and this indicates some change in failure mechanism. It is proposed that, at high stress amplitudes, crack initiation occurs rapidly in the surface, almost irrespective of the presence or not of a coating.

Particularly in the case of light alloys, once cracks are present at the surface, these will proceed into the substrate at an accelerated rate. When a crack tip approaches a plastically weaker material (i.e. having a lower yield strength), the near-tip energy release rate increases, effectively amplifying the crack tip driving force [60]. As the applied stress decreases, the higher fracture toughness of the Ti–6Al–4V substrate limits potential crack growth; however, cracks can still rapidly grow through the brittle TiN layer as this is unable to withstand the substrate elastic strain (Fig. 10a). Once the crack reaches the substrate, its larger size and therefore higher stress intensity promotes continued growth, leading to fracture.

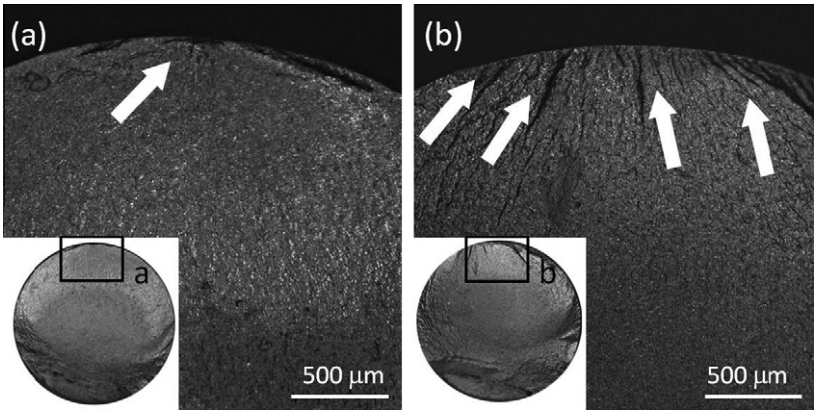

Fig. 9. Stereo microscope fractographs of TiN-coated samples tested at stress amplitudes of (a) 640 MPa and (b) 800 MPa. Arrows indicate crack initation site/s.

Thus, a more drastic drop in fatigue life is observed in the high-cycle fatigue region for TiN-coated (compared to untreated) material.

In the case of duplex treated samples, the prior nitrogen diffusion process counters the premature fatigue failure and these samples exhibit a performance much closer to that of the as-received material. This improvement, when compared to only TiN-coated samples, relates both to the surface strengthening described earlier and improved coating load-support. As a result, the overall presence of cracks in the coating is largely reduced (compare for example Fig 10b and c) but also crack fronts reaching the nitrided surface can be blocked from further advancement (Fig. 10d). Irrespective of the improved adhesion strength of the coating with the nitrided substrate, the nitrided surface creates a sufficiently important obstruction to crack propagation as to allow some deflection of the crack along the coating-substrate interface.

3.6. Effect of surface roughening

The above discussion however fails to take into consideration another aspect which has potential implications for the changes observed in fatigue strength. Cracks in defect-free materials predominantly originate from a free surface and therefore higher surface roughness values tend naturally to be associated with reduced fatigue life. Thus, surface engineering processes which increase significantly the surface roughness also need careful monitoring of their effects in this respect. Invariably, all diffusion processes discussed here have been found to increase the surface roughness to some extent. In most typical 'precision' engineering surface finish (with an R_a value of, say, 0.2–0.4 μm), these roughening effects are still relatively small. On the other hand, a 'superfinished' surface (as might be introduced to a bearing, to mitigate rolling-contact fatigue) would typically present a surface finish in a range an order of magnitude lower than this, where such roughening effects cannot necessarily be neglected.

Amongst the samples tested, LV-TPN(HT) samples had the highest R_a value of 0.18 ± 0.01 μm, while all other samples had R_a values between 0.04 μm and 0.09 μm – the minimum value being equivalent to the polished condition. The annealed and TiN-coated samples had statistically identical R_a values to the untreated batch; however, the drop in fatigue strength was largest between these two. Similarly, while the LHV-TPN samples had an R_a value around 30% higher than that of LV-TPN samples, the fatigue performance of the former was significantly better. Clearly, the roughness measurements do not correlate with the fatigue results presented in Section 3.2. The relatively small increase in surface roughness does not significantly influence the rotating-bending fatigue test

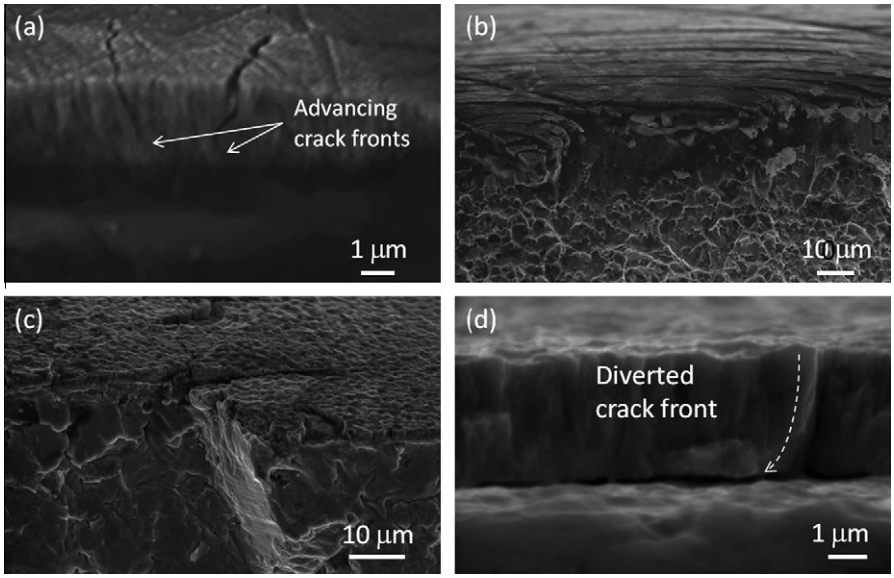

Fig. 10. SEM fractographs of an only TiN coated sample (a and b) and an LHV–TPN–TiN sample (c and d) tested at 640 MPa and 840 MPa, respectively.

results. It can thus be concluded that the negative effects (if any) of diffusion treatment surface roughening are overshadowed by the positive mechanisms already discussed. This is associated with the fact that the maximum roughness 'valley depths' resulting from the different degrees of process-induced roughening were maintained below the size of the principal crack initiation sites present in the samples [48]. In other words, it is suggested that the surface roughness should be below some threshold value, so that crack nucleation is not a function of surface topography. In the absence of residual stress, the limiting R_a value (such that surface roughness has a negligible effect on fatigue life) is claimed to be $\leqslant 0.1$ μm [48]. This theoretical threshold value is likely to be significantly higher under conditions of compressive residual stress. This is confirmed in our work by the fact that the only sample with an R_a value higher than this threshold was LV-TPN(HT) – but, with a high level of compressive residual stress, this sample showed almost identical fatigue response at all stress levels to the LHV-TPON (with comparatively low compressive stress – and an R_a value of only 0.076 ± 0.01 μm). Thus, for samples where surface crack nucleation is dominant, this has to be related to the comparative ease of slip band formation in cyclic loading, where ridges and grooves (known as slip-band 'extrusions' and slip-band 'intrusions', respectively) can be generated [61].

4. Conclusions

Ti–6Al–4V has been nitrided and oxy-nitrided (using a triode-enhanced plasma diffusion treatment) and sequentially coated with TiN using EB-PAPVD under similar triode-plasma conditions. Surface nano- and micro-indentation hardness measurements show a significant increase in hardness to depths of between 30 and 60 μm below the surface, following treatment for 4 h at 700 °C. A number of rotating-bending fatigue tests were carried out for several variants of the triode plasma diffusion treated and duplex diffusion/coating treated samples, in order to assess potential effects on the material's resistance to cyclic loading. The results obtained show that the sample fatigue life depends on the bulk microstructure and diffusion process parameters.

In this study, selection of an appropriate triode plasma diffusion process (carried out at 700 °C) was shown to be capable of matching the original high endurance limit of a very fine-grained, non-annealed microstructure. This has been observed despite the occurrence of substantial annealing – but with negligible grain growth – of the bulk microstructure during treatment. Conversely, taking an annealed substrate microstructure as the baseline, it is possible to improve substantially the fatigue performance – due in significant measure to the compressive stress state created by the presence of nitrogen and/or oxygen located primarily in interstitial solid solution. The results also show that LHV-TPN treatments are the best candidates for use in applications were fatigue performance is considered critical.

Furthermore, the triode plasma treatments used in this work do not in general seem to create a sufficiently roughened surface (as might typically be associated with conventional thermal – or 'diode' plasma – diffusion treatments) so as to have a deleterious effect on the fatigue life of most engineering components (where the initial surface R_a of the component is generally significantly higher than that which might result from any diffusion treatment applied).

The results presented here prove that the deposition of a hard PVD layer alone is detrimental for fatigue endurance. This is associated with a lack of load-support offered by the untreated Ti substrate. A duplex treatment/coating combination provides better load-support, and a functional grading of both hardness and elastic modulus, increasing the resistance to surface strains developed by the applied cyclic stresses. An approximate 16% improvement in fatigue endurance is measured when comparing duplex LV-TPN/TiN with the annealed samples. Therefore, the use of a duplex treatment intended for the enhancement of wear resistance of Ti–6Al–4V (consisting of a low-pressure intensified-plasma diffusion process followed by a ceramic PVD layer) has also been proved capable of maintaining the intrinsically good fatigue properties of the alloy.

This study also demonstrates that the fatigue strength of Ti–6Al–4V is very susceptible to changes in bulk microstructure; it is therefore recommended that all fatigue-related studies of surface modification treatments for such materials should clearly indicate the bulk characteristics of the material tested both before and after treatment (and that data where such information is not given be treated with caution). Only then can sound conclusions be drawn on the net effects of any surface engineering process applied. Clearly, the use of materials which are metallographically more 'coarse' (e.g. in an annealed & furnace-cooled condition) facilitates easier measurement of the relative fatigue response before and after surface treatment.

Acknowledgements

The authors gratefully acknowledge financial support for this research work from the UK Technology Strategy Board, under Technology Programme Project TP/22076, in collaboration with Tecvac Ltd., NMB-Minebea UK Ltd., and Airbus UK.

References

[1] Wierzchon T, Fleszar A. Surf Coat Technol 1997;96:205–9.
[2] Wiklund U, Hutchings IM. Wear 2001;251:1034–41.
[3] Fu Y, Loh NL, Batchelor AW, Liu D, Zhu X, He J, et al. Surf Coat Technol 1998;106:193–7.
[4] Leyland A, Fancey KS, Matthews A. Surf Eng 1991;7(3):207–15.
[5] Matthews A, Leyland A, Dorn B, Stevenson PR, Bin-Sudin M, Rebholz C, et al. J Vac Sci Technol A 1995;13(3):1202–7.
[6] Wilson A, Leyland A, Matthews A. Surf Coat Technol 1999;114:70–80.
[7] Matthews A, Leyland A. Surf Coat Technol 1995;71:72–88.
[8] Bin-Sudin M, Leyland A, James AS, Matthews A, Housden J, Garside B. Surf Coat Technol 1996;81:215–24.
[9] Cassar G, Avelar-Batista Wilson JC, Banfield S, Housden J, Matthews A, Leyland A. Wear 2010;269:60–70.
[10] Costa MYP, Cioffi MOH, Venditti MLR, Voorwald HJC. Proc Eng 2010;2:1859–64.
[11] Wilson A, Matthews A, Housden J, Turner R, Garside B. Surf Coat Technol 1993;62:600–7.
[12] Ebrahimi AR, Zarei F, Khosroshahi RA. Surf Coat Technol 2008;203:199–203.
[13] Shibata H, Tokaji K, Ogawa T, Hori C. Fatigue 1994;16:370–6.
[14] Leyland A, Fancey KS, James AS, Matthews A. Surf Coat Technol 1990;41:295–304.
[15] Donachie Jr MJ. Titanium: a technical guide. 2nd ed. ASM International; 2007.
[16] BS EN ISO 4545-1, Metallic materials – Knoop hardness test – Part 1: Test method; 2005.
[17] BS 3518: Part2, Methods of fatigue testing: Part 2 Rotating bending fatigue tests; 1962.
[18] BS ISO 12107, Metallic materials – fatigue testing – statistical planning and analysis of data; 2003.
[19] Kashaev N, Stock HR, Mayr P. Met Sci Heat Treat 2004;46(7–8):294–8.
[20] Meletis EI. Surf Coat Technol 2002;149:95–113.
[21] Winters Harold F. J Appl Phys 1972;43(11):4809–11.
[22] Wood FW, Paasche OG. Thin Solid Films 1977;40:131–7.
[23] Unnam J, Shenoy RN, Clark RK. Oxid Met 1986;26(3/4):231–52.
[24] Cassar G. Ph.D thesis. UK: The University of Sheffield; 2011.
[25] ASTM E468-90, Standard practice for presentation of constant amplitude fatigue test results for metallic materials; 1998.
[26] Hall JA. Int J Fatigue 1997;19(1):523–37.
[27] ASM Handbook, vol. 19. Fatigue and fracture. ASM International; 1996.
[28] Ashrafizadeh F. Surf Coat Technol 2003;173–174:1196–200.
[29] Bell T, Bergmann HW, Lanagan J, Morton PH, Staines AM. Surf Eng 1986;2(2):133–43.
[30] Lütjering G, Williams JC. Titanium. 2nd ed. New York: Springer; 2007.
[31] Nalla RK, Boyce BL, Campbell JP, Peters JO, Ritchie RO. Metall Mater Trans A 2002;33A:899–918.
[32] Leyens C, Peters M. Titanium and titanium alloys. Weinheim: Wiley-VCH; 2005.
[33] Vardiman RG, Kant RA. J Appl Phys 1982;53(1):690–4.

[34] Rodriguez D, Manero JM, Gil FJ, Planell JA. J Mater Sci – Mater Med 2001;12:935–7.
[35] Major B, Golebiewski M, Wierzchon T. J Mater Sci Lett 2002;21:1289–92.
[36] Raveh A, Bussiba A, Bettelheim A, Katz Y. Surf Coat Technol 1993;57:19–29.
[37] Zhecheva A, Sha W, Malinov S, Long A. Surf Coat Technol 2005;200:2192–207.
[38] Rie KT, Stucky T, Silva RA, Leitao E, Bordji K, Jouzeau JY, et al. Surf Coat Technol 1995;74–74:973–80.
[39] Sobiecki JR, Wierzchoń T. Surf Coat Technol 2006;200:4363–7.
[40] Guclu FM, Cimenoglu H, Kayali ES. Mater Sci Eng C 2006;26:1367–72.
[41] ASM Handbook, vol. 3. Alloy phase diagrams. ASM International; 1996.
[42] Montanari R, Costanza G, Tata ME, Testani C. Mater Charact 2008;59:2428–32.
[43] Genel K, Demirkol M, Capa M. Mater Sci Eng A 2000;297:207–16.
[44] Fitzpatrick ME, Fry AT, Holdway P, Kandil FA, Shackleton J, Suominen L. Determination of residual stresses by X-rays diffraction – measurement good practice guide 52. Teddington: NPL; 2002.
[45] Agarwal N, Khan H, Avishai A, Michal G, Ernst F, Heuer AH. Acta Mater 2007;55:5572–80.
[46] Michal GM, Ernst F, Khan H, Cao Y, Oba F, Agarwal M, et al. Acta Mater 2006;54:1597–606.
[47] Drechsler A, Kiese J, Wagner L. In: Proceedings of the 7th international conference on shot peening, Warsaw, Poland; 1999. p. 145–52.
[48] Novovic D, Dewes RC, Aspinwall DK, Voice W, Bowen P. Int J Mach Tool Manu 2004;44:125–34.
[49] Wagner L. Mater Sci Eng A 1999;A263:210–6.
[50] Torres MAS, Voorwald HJC. Int J Fatigue 2002;24:877–86.
[51] Holmberg K, Matthews A. Coatings tribology – properties mechanisms techniques and applications in surface engineering. 2nd ed., Tribology and Interface Engineering Series No. 56. Amsterdam: Elsevier Science; 2009.
[52] Erdemir A, Hochman RF. Surf Coat Technol 1988;36:755–63.
[53] Baragetti S, La Vecchia GM, Terranova A. Int J Fatigue 2005;27:1541–50.
[54] Laz PJ, Hillberry BM. Int J Fatigue 1998;20(4):263–70.
[55] Baragetti S, Terranova A. SID 2005;1(4):267–76.
[56] Nascimento MP, Souza RC, Pigatin WL, Voorwald HJC. Int J Fatigue 2001;23:607–18.
[57] Stone DS, Yoder KB, Sproul WD. J Vac Sci Technol A 1991;9:2543–7.
[58] Su YL, Yao SH, Wei CS, Wy CT. Thin Solid Films 1998;315:153–8.
[59] Puchi-Cabrera ES, Matinez F, Herrera I, Berrios JA, Dixit S, Bhat D. Surf Coat Technol 2004;182:276–86.
[60] Sugimura Y, Lim PG, Shih CF, Suresh S. Acta Metall Mater 1995;43(3):1157–69.
[61] Dieter GE. Mechanical metallurgy. London: McGraw-Hill Book Company; 1998.